Quaternary Polarization-Multiplexed Subsystem for High-Capacity IM/DD Optical Data Links

Estaran Tolosa, Jose Manuel; Usuga Castaneda, Mario A.; Porto da Silva, Edson; Piels, Molly; Iglesias Olmedo, Miguel; Zibar, Darko; Tafur Monroy, Idelfonso

Published in:
Journal of Lightwave Technology

Link to article, DOI:
10.1109/JLT.2015.2397010

Publication date:
2015

Document Version
Publisher's PDF, also known as Version of record

Quaternary Polarization-Multiplexed Subsystem for High-Capacity IM/DD Optical Data Links

José Estarán, *Student Member, IEEE*, Mario A. Usuga, *Member, IEEE*, Edson Porto da Silva, *Student Member, IEEE*, Molly Piels, *Member, IEEE*, Miguel Iglesias Olmedo, *Student Member, IEEE*, Darko Zibar, *Member, IEEE*, and Idelfonso Tafur Monroy, *Senior Member, IEEE*

(Invited Paper)

***Abstract*—We demonstrate for the first time an intensity-modulated direct-detection link using four states of polarization. The four data-independent tributaries are each assigned distinct states of polarization to enable the receiver to separate the signals. Polarization rotation due to propagation over optical fiber is tracked and compensated with simple digital signal processing in Stokes space. Transmission below the forward error correction limit is shown for maximum net bitrates of 100 Gb/s (4 × 27 GBd) and 120 Gb/s (4 × 32 GBd) over 2-km standard single-mode fiber at a center wavelength of 1550 nm.**

***Index Terms*—100G, digital signal processing, direct detection (DD), intensity modulation (IM), polarization, Stokes space.**

I. Introduction

POLARIZATION multiplexing in the optical domain is a critical technology in current coherent optical transmission systems, as it doubles the amount of information traveling through a single fiber. This idea had been considered since polarization diversity receivers were proposed in 1990 [2], but was not commercially feasible until efficient digital signal processings (DSPs) was presented in 2005 [3]. Analogously, the use of polarization diversity in intensity modulation and direct detections (IM/DDs) optical data links was proposed in 1986 [4], but commercial applications have not been developed yet.

IM/DDs is still the predominant technology in optical data links covering up to tens of kilometers, where simple and cost-effective systems have prevailed. Bitrate requirements in IM/DD links are so far fulfilled by means of parallel optics and wavelength division multiplexings (WDMs); however, the burdensome upgrade requirements of those approaches makes it difficult to keep pace with growing capacity demand. Most research efforts focus on spectrally efficient advanced modulation formats compatible with IM/DDs optics. High-rate baseband demonstrations include [5], [6], where the improvement in spectral efficiency (SE) is achieved with 4-ary pulse amplitude modulation (4-PAM) and duo-binary (first form of partial response modulation) respectively. More sophisticated advanced modulation formats are explored in [7]–[9], with the use of discrete multitone modulation; and in [10] and [11], where passband carrierless amplitude phase modulation is employed. However, the downside with these approaches is that the gains in SE are often overshadowed by the computational load of the processing algorithms and/or the restricted scalability of the transceiver structures.

In this context, polarization diversity has recently arisen as a feasible means to enhance current IM/DD systems and relax their previously mentioned limitations. For instance in *self-coherent* direct-detection systems, the data and the remote frequency pilot tone(s) are transmitted in a user-defined configuration that may exploit the extra dimensionality to increase the SE and/or simplify the receiver structure [12]–[16]. Despite these improvements, polarization-multiplexed *self-coherent* IM/DD systems have not yet reached a satisfactory solution that conveniently balances the triple trade-off between SE, the complexity of the transmitter and receiver structures, and computational load. Alternatively, polarization-multiplexed *incoherent* IM/DD systems represent a fundamentally simpler and more spectrally efficient approach, where the major challenge lies in enabling compact and robust polarization demultiplexing and channel's polarization-dependent distortions compensation without explicit phase reference after photodetection. Recent contributions in this line include [17], where the author presents a novel DSP algorithm which, by manipulating the Stokes vectors of the received signal, supports the simultaneous transmission of two orthogonal states of polarization (SOP). Based on the receiver structure introduced in [17] and low-complexity DSP, [18] and [19] show simulated high-rate fiber transmissions (up to 100 Gb/s) of multi-level optical signals directly designed in the three-dimensional (3-D) Stokes space. Concerning experimental demonstrations of *incoherent* polarization-multiplexed IM/DD systems, [20] shows 10-km 1310-nm transmission over standard single-mode fiber (SSMF) of dual-polarization 4-PAM. The Stokes parameters are opto-electrically obtained through a six-photodiode Stokes receiver (see [16]), and a multi-tap adaptive equalizer is employed for polarization demultiplexing and signal equalization.

In this paper, we report on a technique for polarization-multiplexed *incoherent* IM/DD systems that goes beyond the state of the art by allowing simultaneous transmission of four independent data streams carried by four different SOP. Additionally, a four-photodiode Stokes analyzer (see [21]) is used at the receiver side, enabling the utilization of a simple 4-SOP

Manuscript received November 2, 2014; revised January 14, 2015; accepted January 22, 2015. Date of publication January 29, 2015; date of current version March 4, 2015. This work was supported in part by the VILLUM FOUNDATION, Søborg, Denmark. This work extends the results presented at the European Conference on Optical Communication, Cannes, France, 21–25 September 2014 [1].

The authors are with DTU Fotonik, Department of Photonics Engineering, Technical University of Denmark, 2800 Kgs. Lyngby, Denmark (e-mail: jome@fotonik.dtu.dk; mauc@fotonik.dtu.dk; edpod@fotonik.dtu.dk; mopi@fotonik.dtu.dk; molm@fotonik.dtu.dk; dazi@fotonik.dtu.dk; idtm@fotonik.dtu.dk).

Color versions of one or more of the figures in this paper are available online at http://ieeexplore.ieee.org.

Digital Object Identifier 10.1109/JLT.2015.2397010

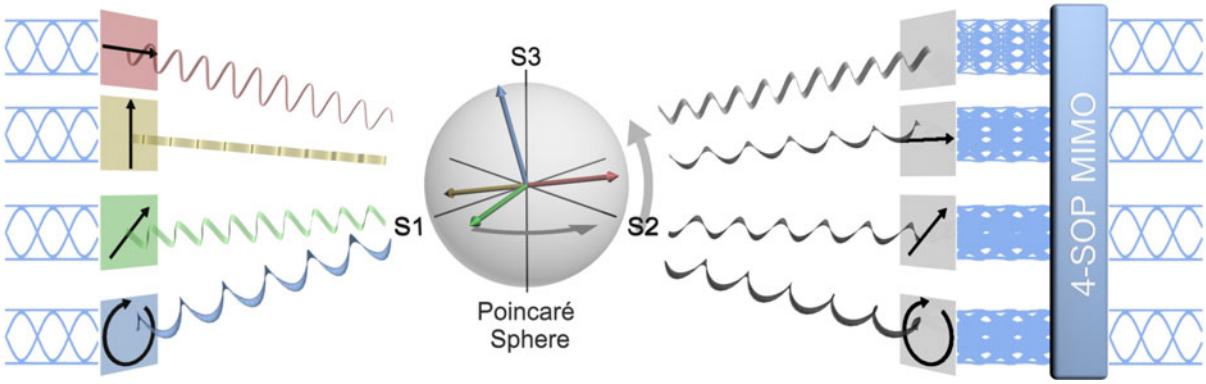

Fig. 1. Conceptual illustration of the proposed quadruple polarization system for IM/DD optical data links.

tracking algorithm for successful data recovery. Experimental demonstration shows successful transmission and demodulation after 2-km SSMF at a rate up to 128 Gb/s at a center wavelength of 1550 nm. This is, to the best of our knowledge, the first time this multi-polarization transmission system is experimentally proven for high-capacity IM/DD fiber-optic data links. The technique has the potential to be used alongside or in place of current existing technologies for capacity increase and simplification of the receiver structure. For example, client-side optical data links using coarse WDMs (CWDM), can quadruple the throughput per CWDM channel without modifying the WDMs hardware. Alternatively, the induced polarization diversity can be used as selective factor instead of pass-band optical filtering.

The remainder of this paper is organized as follows. Section II describes the architecture of the quaternary polarization-multiplexed IM/DD transmission subsystem; highlighting relevant aspects of the transmitter, the receiver and the DSPs chain. Section III provides details on the experimental demonstration; encompassing a description of testbed where the principle was validated, and the presentation and discussion on the results. Finally, Section IV summarizes and concludes our work.

II. Quaternary Polarization Multiplexing

The traditional approach to polarization multiplexing is to encode data streams into two linear and orthogonal polarization components (often referred to as *X* and *Y*). The orthogonality condition prevents optical interference between the polarized waves in the absence of channel-induced distortion (or after compensation); however, it does not limit a multi-polarization system in number of channels to two. Herard and Lacourt [4] were the first to take advantage of this fact in an optical communication system, experimentally demonstrating a free-space IM/DD link with three SOPs and analog demultiplexing. This was followed by Herard and Lacourt [22], with an extended theoretical analysis accounting for the impact of various factors including polarization mode dispersion and mode coupling on the system's performance. At that time, no more than three SOPs were used for simultaneous data transmission in IM/DD scenarios, and no algorithm for real-time polarization tracking was presented. In this work, we demonstrate for the first time a quaternary polarization-multiplexed (4-SOP) IM/DD system in a transmission medium in which polarization mixing/rotation occurs, i.e., optical fiber. The inclusion of circular SOPs along with full operation in Stokes space enabled both the addition of a fourth SOP and polarization rotation compensation without the need for phase information.

The next sections describe the proposed 4-SOP system, implementation details of both transmitter and receiver structures, and the DSP chain.

A. Conceptual Description

The proposed 4-SOP system is illustrated conceptually in Fig. 1. Four independently intensity-modulated optical signals in four different SOPs are simultaneously transmitted over SSMF, where the polarization rotates over time [23] (indicated by the vectors in the Poincaré sphere, Fig. 1). At the receiver, the components along SOPs *X*, 45° and right circular (*RC*) (or orthogonal counterparts) of the distorted signal are detected, together with the instantaneous total intensity in a standard Stokes analyzer [21]. Subsequently, polarization rotation compensation, demultiplexing and demodulation (processes encompassed within *4-SOP MIMO* in Fig. 1) are performed in the digital domain.

B. Mathematical Description

In matrix form, the system up to photodetection (inclusive) can be expressed as:

$$\mathbf{Out} = \mathbf{H_{sys}}\ \mathbf{In}, \tag{1}$$

where $\mathbf{H_{sys}}$ is an $N \times N$ matrix, with N equal to the number of independent transmitted SOPs, which includes both the channel distortions and the pre-defined input-output SOP configuration. $\mathbf{In}$ and $\mathbf{Out}$ constitute the transmitted and received signals respectively. $\mathbf{In}$ is constructed with the N independently modulated intensity waveforms. $\mathbf{Out}$ is composed of the observed four system outputs after photodetection, and it results from the transformation of the transmitted intensity signals through $\mathbf{H_{sys}}$.

Despite the complex nature of the Jones calculus, the real transfer function of the proposed 4-SOP IM/DD system ($\mathbf{H_{sys}}$) can be readily calculated from the normalized Jones vectors[1]

[1]Its mathematical expression is given by $\mathbf{v} = \begin{pmatrix} \cos\theta & e^{i\phi}\sin\theta \end{pmatrix}$, where θ is the rotation angle of the propagating field with respect to the reference orthogonal polarization components *X* and *Y*; and ϕ indicates their phase difference (relative phase).

of the transmitted and received SOP sets in two steps. First the field transfer function is calculated:

$$\mathbf{G} = \begin{pmatrix} \mathbf{v}_{RX1} \\ \mathbf{v}_{RX2} \\ \mathbf{v}_{RX3} \\ \mathbf{v}_{RX4} \end{pmatrix} \mathbf{H_{dist}} \begin{pmatrix} \mathbf{v}_{TX1}^T & \mathbf{v}_{TX2}^T & \mathbf{v}_{TX3}^T & \mathbf{v}_{TX4}^T \end{pmatrix}, \quad (2)$$

where $\mathbf{v}_{TXj}$ and $\mathbf{v}_{RXj}$ are the 1×2 normalized Jones vectors of the jth transmitted and received SOPs, respectively, and $\mathbf{H_{dist}}$ is the 2×2 Jones matrix that represents the linear distortions undergone by the field along propagation over fiber. Second, the intensity system matrix is obtained from $\mathbf{G}$ with the following Hadamard product:

$$\mathbf{H_{sys}} = \mathbf{G} \circ \mathbf{G}^*. \quad (3)$$

In the absence of channel distortions or after their compensation, $\mathbf{H_{sys}}$ strictly describes the transfer function of the ideal 4-SOP transmission system (introduced in Section II-C as the *mapping matrix*). In this case, if $\mathbf{v}_{TXj} = \mathbf{v}_{RXj}\ \forall j$ and when linear SOPs are used, $\mathbf{H_{sys}}$ can be conveniently constructed by direct evaluation of Malus's law[2] [4].

It is apparent from Eq. (1) that $\mathbf{H_{sys}}$ must be invertible in order to make demultiplexing possible. Because the channel properties cannot be changed as part of the design procedure, careful choice of transmitted and received SOPs ($\mathbf{v}_{TXj}$ and $\mathbf{v}_{RXj}$) is the only method to assure the existence of $\mathbf{H_{sys}^{-1}}$. By inserting Eq. (2) into Eq. (3) for different SOP configurations, the reversibility of $\mathbf{H_{sys}}$ can be studied under the assumption of perfect compensation of the channel distortions (i.e., $\mathbf{det}(\mathbf{H_{sys}}) \neq 0$ for $\mathbf{H_{dist}} = I_2$).

C. Transmitter

Recalling the findings in [4]: when linear SOPs are used as the selective agents for signal (de)multiplexing in an IM/DD system, the maximum achievable diversity equals three. When this limit is exceeded with extra linear SOPs, the three characteristic parameters of the carriers' polarization (amplitude of the projections on the perpendicular polarization planes and rotation angle) cannot be calculated from the received intensities without ambiguity because they are not mutually independent [4], [22]. This leads to an impractical system with irreversible generation process and then, to the misconception that no more than three SOPs can be jointly transmitted and demultiplexed.

Scaling the system beyond three polarizations requires the aggregate SOP to be described by strictly more than three independent parameters. Mathematically, this allows the construction of the characteristic matrix (whose coefficients are associated with physically meaningful independent variables) of a consistent system of more than three equations with a unique solution. This matrix is referred as *mapping matrix* and its inverse as *demapping matrix* ($\mathbf{H_{sys}}$ and $\mathbf{H_{sys}^{-1}}$ in Section II-B). In this work, the four transmitted Jones vectors (see $\mathbf{v}_{TXj}$ in Eq. (2)) employed in the experimental demonstration which enabled the existence of the *demapping matrix* were *X*, *Y*, 45° and left circular (*LC*):

$$\mathbf{Tx} = \begin{array}{c} \\ X \\ 45 \\ Y \\ LC \end{array} \begin{array}{c} \begin{array}{cc} X & Y \end{array} \\ \begin{pmatrix} 1 & 0 \\ \cos\frac{\pi}{2} & \sin\frac{\pi}{4} \\ 0 & 1 \\ \cos\frac{\pi}{4} & i \cdot \sin\frac{\pi}{4} \end{pmatrix} \end{array}. \quad (4)$$

From Eq. (4), it is clear that we indirectly exploit the optical phase as independent parameter by encoding part of the information on a circular SOP. Operating on the optical phase through SOP manipulation avoids the use of complex and costly coherent receivers. This particular configuration (along with the corresponding one at the receiver side) makes demultiplexing possible for up to four different SOPs that now can be simultaneously transmitted over the same medium.

Besides the conditions for assuring the reversibility of the multiplexing process, the choice of transmitted SOPs directly depends on the approach for compensating the channel-induced distortions; which, in turn, defines the final receiver design. This is discussed in the next section.

D. Receiver

During propagation over short-reach fiber links, the transmitted polarization undergoes various distortions. Joint compensation of such detrimental effects demands acting on all four characteristic parameters of the received signal's time-varying SOP. Consequently, provided that phase information is lost after opto-electrical conversion, a quaternary polarization-diversity receiver is necessary irrespective of the multiplexing dimensionality. This represents the first rule for the receiver design of the proposed polarization-multiplexed IM/DD system, being the 4-SOP setting the only 100% hardware efficient (four independent inputs by four photodetectors). The simplest structure for the 4-SOP direct-detection receiver comprises a one-to-four power splitter prior to a fixed set of polarizers, which provide the intended polarization diversity between the various signal copies. Each of the branches ends with respective photodetectors for subsequent digitization and processing in the digital domain (see Section II-E).

It is noteworthy that the polarization filtering stage constitutes the only (optical) processing variable at the receiver, becoming the sole degree of freedom for manipulating the data before acquisition. Thereby, its concrete configuration and its relation with the transmitted SOPs, have a relevant influence on the selection and simplicity of the DSP algorithm for polarization tracking and demultiplexing. Two configuration options are considered here.

1) *Option 1:* In this mode, transmitter and receiver SOPs are the same ($\mathbf{v}_{TXj} = \mathbf{v}_{RXj}\ \forall j$). Pre-defined training sequences are transmitted on each of the four distinct SOPs, the channel matrix is then estimated through direct calculation of the input-output transfer function. This transfer function includes the channel-induced polarization distortions and, alternatively, the static *mapping matrix* (see Section II-C).

[2]The total intensity of a light beam going through a perfect polarizer is dependent on the incident angle θ as follows: $I_{\mathrm{out}} = I_{\mathrm{in}} \cos^2\theta$.

Despite the conceptual simplicity and robustness, impairment compensation and demultiplexing require periodic inversion of the channel matrix, greatly increasing the processing load. Moreover, the temporal discontinuity of the channel estimation prevents the system from tracking fast polarization changes, and establishes a trade-off between the effective bitrate and the accuracy of the compensation.

2) *Option 2:* Three of the polarizers at the receiver are aligned to *X* or *Y*, *45°* or *135°* and *RC* or *LC* respectively. The remaining photodiode captures the instantaneous total power (no polarizer). This general structure is named *Stokes analyzer*, and enables the determination of the Stokes parameters from the measured intensities through linear transformation:

$$\begin{aligned} S0 &= I_{\mathrm{TOTAL}} \\ S1 &= 2I_{X/Y} - S0 \\ S2 &= 2I_{45/135} - S0 \\ S3 &= 2I_{RC/LC} - S0. \end{aligned} \tag{5}$$

This approach aims (simplifying) the construction of the Stokes parameters in the subsequent processing stage (digital in this work). Their direct manipulation makes possible the exploitation of the good properties of the Stokes space for SOP characterization and demultiplexing [24]. However, operating in the Stokes space also implies a change to a coordinate system in which orthogonal SOPs differ from the ones in the standard real space. This observation turns of great importance in the proposed system, where four interfering SOPs are simultaneously transmitted. Orienting the transmitted polarized light beams toward orthogonal Stokes coordinates avoids undesired intermediate transformations (extra processing) and greatly facilitates symbol detection (see Section II-E). This is the reason for the particular set of transmitted Jones vectors indicated in Section II-C, Eq. (4).

For this study, the polarizers of the *Stokes analyzer* are aligned to *X*, 135° and *RC*. The corresponding Jones vectors describing the polarization of the field at the input of the Stokes analyzer's branches are ($\mathbf{v}_{RXj}$ in Eq. (2)):

$$\mathbf{Rx} = \begin{array}{c} \\ - \\ X \\ 135 \\ RC \end{array} \begin{array}{c} \begin{array}{cc} X & Y \end{array} \\ \begin{pmatrix} 1 & 1 \\ 1 & 0 \\ \cos\frac{3\pi}{4} & \sin\frac{3\pi}{4} \\ \cos\frac{\pi}{4} & -i\cdot\sin\frac{\pi}{4} \end{pmatrix} \end{array}. \tag{6}$$

The SOP configuration described by Eqs. (4) and (6) maximizes the number of orthogonal (in the Stokes space) transmitted SOPs while assuring the existence of the *demapping matrix*; and minimizes the order of the resulting multilevel signals after photodectection under perfect alignment conditions. The latter is convenient for the initial system optimization.

As mentioned, the required digital processing depends strongly (structure and computational load) on the concrete the SOP-wise design of the system. The following analyses and results relate to the *Option 2* architecture, whose potential allows for blind tracking and demultiplexing of the propagated SOPs without matrix inversion. These and other relevant aspects of the DSP chain are introduced in the next section.

E. Digital Receiver—Stages and Considerations

The DSP chain described in this section relates to one of the possible solutions for satisfactory pre-FEC data demodulation in the proposed 4-SOP IM/DD subsystem; and it includes what the authors consider to be the necessary stages with the optimum succession order. For the readers' convenience, the schema of the full DSP chain is included in appendix.

The subdivision of the DSP chain is composed of three blocks: (i) general front-end correction, (ii) polarization tracking plus channel rotation compensation and (iii) demultiplexing. The first block accounts for the always-necessary signal conditioning:

1) *Resampling:* The four captured sequences are resampled to the minimum number of integer samples per symbol.
2) *Filtering:* Out-of-band noise and (possible) undesired spectral components caused by signal–signal beating in the photodetector are attenuated for signal-to-noise ratio (SNR) maximization.

The second block covers every action related to the polarization tracking/demultiplexing algorithm. These include individual corrections of the measured intensities, which relate to expectable penalties due to the experimental implementation. The target here is maximizing the accuracy of the subsequent calculation of Stokes parameters (see Section II-D, Eq. (5)).

1) *Time skew:* Skews originating both at the transmitter and receiver sides have different though critical impact on the appropriate functioning of the system. The skew at the transmitter cannot be easily corrected by DSP (at the receiver) and it requires precise symbol synchronization between the independent signal generators up to the fiber input. It determines the quality of the received multilevel signals, affecting both the cleanliness of the levels and the sampling-point deviation tolerance.

   The skew at the receiver does not alter the multilevel signal's quality as described above, but their respective time alignment. Because the calculation of all the Stokes parameters depends on the measured instantaneous total power, misalignments of sufficient magnitude between symbol periods can severely affect the performance and even prevent demodulation. Additionally, given that the received power is not affected by the considered polarization-dependent impairments, *S0* becomes a robust convenient reference for common optimum sampling selection irrespective of the severity of the distortion. This underscores the need for accurate symbol synchronization across all the branches of the *Stokes analyzer*, where preceding frame/coarse synchronization is understood. Note that, unlike transmitter skew, the receiver's skew is independent of the baudrate and the chromatic dispersion even when independent laser sources are employed.
2) *Scaling:* The ratios between the measured intensity waveforms are crucial for determining the mixing coefficients. Performing individual power (or amplitude)

normalization of the captured intensities is a mistake that surely leads to incorrect impairment compensation and demultiplexing. It follows that differences in the responsivities of the four photodiodes are detrimental and need to be equalized. Variations of the respective responsivities reflect as wrong proportions among the signal amplitudes that yield distorted eye diagrams when combined for creating the Stokes parameters.

3) *DC offset:* Different photodiodes may also show disparate output dc components for the same input optical power. Even with equalized responsivities, uncompensated dc components may accumulate when calculating the Stokes parameters, producing asymmetric and/or offseted eyediagrams. Unless addressed, this effect modifies the optimum decision boundaries, hence compromising the performance and stability of the blind SOP demultiplexing algorithm.

It is possible that the response of the photodiodes vary with the input power level. In such case, scaling factors and dc compensation values should be adjusted according to the received optical power for improved SOP tracking and symbol error rate. After the aforementioned corrections, the transformation of the intensities to Stokes parameters is performed as indicated in Eq. (2). From this step on, the DSP operates on the Stokes space.

4) *Timing recovery and sampling point* Standard Gardner timing recovery and maximum-variance decimation is performed on the four Stokes parameters [25]. As mentioned in the *Skew* description, the invulnerability of *S0* to polarization-dependent distortions enables employing it as robust reference for common optimum sampling point and phase correction estimation. This is conditioned to precise skew compensation and negligible deviation between sampling instants across the four branches.

The Mueller matrix of the end-to-end channel response is blindly estimated in the next stage ($\mathbf{M_{dist}}$, and $\mathbf{H_{dist}}$ in Jones calculus[3]). Because polarization distortions along propagation reflect as 3-D rotations of the Stokes space coordinate system, the channel's Mueller matrix reduces to the standard rotator form:

$$\mathbf{M_{dist}} = \begin{pmatrix} 1 & 0 & 0 & 0 \\ 0 & S_{11} & S_{12} & S_{13} \\ 0 & S_{21} & S_{22} & S_{23} \\ 0 & S_{31} & S_{32} & S_{33} \end{pmatrix}, \tag{7}$$

where S_{ij} for $i, j \in \mathbb{Z}$ are real-valued coefficients which quantize the normalized coupling factors between the Stokes parameters i and j.

The following algorithm to find $\mathbf{M_{dist}}$ is inspired in the work in [17], where a blind method for tracking a single Stokes vector was proposed; hence permitting polarization rotation compensation of two orthogonal Jones vectors in IM/DD systems. The novelty introduced in this work resides in the capability to measure the channel-induced rotations on all the three Stokes vectors (i.e., $S_{ij}\ \forall i, j$). This extension enables simultaneous, simple and blind polarization tracking and demultiplexing beyond two SOPs which, additionally, are not restricted to be orthogonal. The next item elaborates on the details of the tracking process. This is supported with Fig. 2, where simulated (colored) histograms of the normalized Stokes parameters *S1* (see Fig. 2(a)) and *S2* (see Fig. 2(b)) are shown for perfect transmitter-receiver SOP alignment. Experimental results (grey) are presented for the sake of comparison. Note that the asymmetry around zero of the histogram in Fig. 2(b) is due to the fact that only the 45° SOP is transmitted and not the 135° counterpart. This contrasts with *S1* given that both *X* and *Y* are employed. In this regard, *S2* and *S3* exhibit similar histograms.

5) *SOP tracking* Zero-power symbol detection is performed prior to the power normalization of the Stokes vectors. The former is done through direct thresholding on *S0*'s lowest-power level. The samples below threshold are demapped to the corresponding bit tuple, and the respective values are removed from the four Stokes sequences. This avoids creating mathematical indeterminations in the following normalization by *S0*.

Normalizing the Stokes vectors by *S0* is a key operation with one main implication: it makes polarized components show maximum power, i.e., they lie on the surface of the Poincaré sphere (green-colored observations in Fig. 2). If the transmitted SOPs are aligned with the polarizers of the *Stokes analyzer*, all their individual power is projected onto the respective (single) Stokes vector in the absence of distortions (green-colored groups of points around ± 1 in Fig. 2). This is the observation governing the tracking algorithm.

The above mentioned distortions in the proposed 4-SOP system can be subdivided into (i) mapping- and (ii) channel-dependent. When mapping independent random data, those instants in which the bit combination excites two or more interfering SOPs simultaneously (e.g., *X* and 45°) will appear as partially polarized components. As these aggregate SOPs are not aligned with the reference coordinates of the *Stokes analyzer*, they will generate additional projections on the orthogonal axes with less than unity power (blue-colored observations in Fig. 2). These power levels hinder the detection of the polarized instants (notice level overlapping in the grey-colored experimental data), which are the reference for the estimation of the channel characteristic matrix as explained in the next paragraph. The separation between the projections of polarized and partially polarized components is increased when the number of orthogonal (in both domains) transmitted SOPs is maximized (subjected to the existence of *demapping matrix*). This underlines the reasoning behind the transmitter-receiver structure used in the present work (see Section II-C matrix 4 and Section II-D matrix 6).

Second, when the channel induces undesired polarization-dependent effects it causes a virtual 3-D rotation of the Stokes-space coordinate system. Consequently, the power

[3]For Jones-to-Mueller conversion: $\mathbf{M} = \mathbf{A}(\mathbf{J} \otimes \mathbf{J}^*)\mathbf{A}^{-1}$, where $\mathbf{M}$ and $\mathbf{J}$ are the Mueller and Jones matrices respectively and $\mathbf{A}$ is given by:

$$\mathbf{A} = \begin{pmatrix} 1 & 0 & 0 & 1 \\ 1 & 0 & 0 & -1 \\ 0 & 1 & 1 & 0 \\ 0 & i & -i & 0 \end{pmatrix}.$$

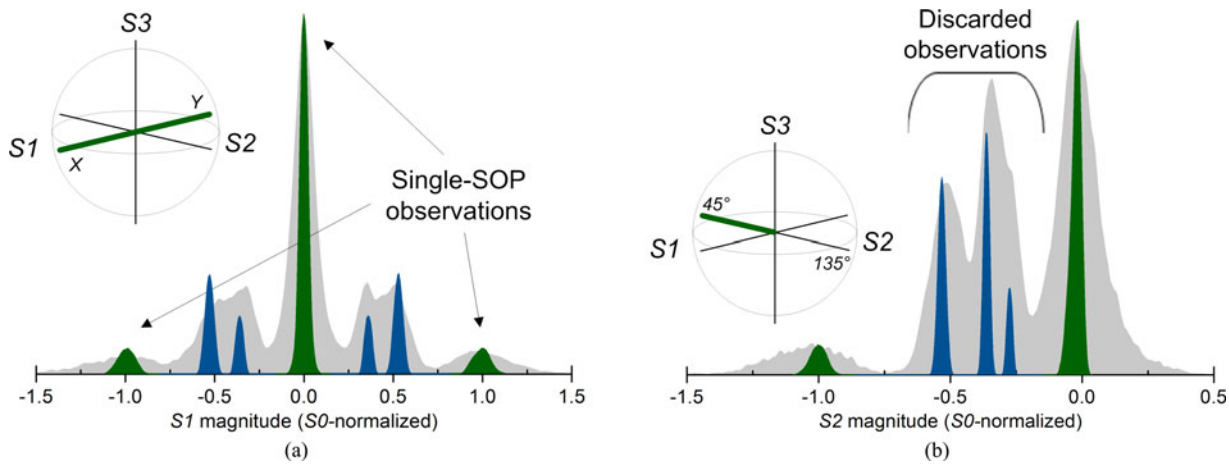

Fig. 2. Histogram of the Stokes parameters *S1* (a) and *S2* (b) normalized by *S0* for perfect transmitter-receiver polarization alignment. In color, simulated data for 40-dB SNR B2B configuration. In grey, experimental results for 4 $\times$ 27 GBd at 6 dBm optical power into the receiver. Insets: Poincaré spheres. The Stokes parameters of both (a) and (b) are highlighted.

of a transmitted polarized light beam is not projected on a single Stokes vector which, instead, spreads among the three dimensions. The absolute deviation from unity power along the intended Stokes vector (together with the leakage on the others) constitutes the error signal magnitude, representing a quantization of the channel-induced polarization-dependent impairments in one of the three dimensions. Note that the calculation of the error signal is based on the relative power deviation with respect to a normalized magnitude, thereby the possibility to run the algorithm directly on payload (blind operation). The sign-sensitive error signal is then included in a standard normalized least mean square (NLMS) adaptive filter calculation. The reader is referred to [17] for detailed mathematical formulation of both NLMS filter update rule and error signal estimation.

The objective of the iterative NLMS process is to converge to a filter that mimics the rotation undergone by the one *Stokes analyzer*'s reference axis being observed. The affected axis/Stokes vector is then de-rotated (see *Channel distortion compensation*), and the transmitted SOPs (exclusively depending on such dimension) can be successfully demultiplexed and demodulated. The process is repeated in series for any two Stokes vectors, where the alternation is triggered by a simple zero-power exception indicating that the orthogonal SOP has been transmitted (green-colored observations around 0 in Fig. 2). Conveniently, the third orthogonal coordinate can be obtained through the cross-product of the previously estimated vectors. After full convergence, the algorithm locks, enabling simple, continuous and blind tracking in the whole Stokes space.

It is worth remarking that the algorithm described here is a tracking tool and, therefore, it needs initialization. The alternatives and main aspects concerning such initialization process are not covered in this paper.

6) *Channel distortion compensation:* During *SOP tracking* the 3-D rotation of the Stokes space as consequence of the distortions induced by the channel is characterized and quantified. Equivalently, a new rotated coordinate system is obtained. Assuming the inability to dynamically change the SOPs at the transmitter/receiver, we need to perform digital de-rotation of the received Stokes vectors. This is generally done by applying the inverse channel matrix, with the consequent increase of the computational cost (which becomes heavier the faster the polarization changes to be tracked become). However, given that rotations do not break the orthogonality condition among the coordinate vectors in the Stokes space, the inverse is readily calculated with standard matrix transposition:

$$\mathbf{M}_{\mathbf{dist}}^{-\mathbf{1}} = \mathbf{M}_{\mathbf{dist}}^{\mathbf{T}} = \begin{pmatrix} 1 & 0 & 0 & 0 \\ 0 & S_{11} & S_{21} & S_{31} \\ 0 & S_{12} & S_{22} & S_{32} \\ 0 & S_{13} & S_{23} & S_{33} \end{pmatrix}. \quad (8)$$

This property, which helps maintain a low computational load, becomes crucial for the implementation feasibility of the proposed 4-SOP IM/DD architecture.

After transposition, the matrix is applied on the received Stokes sequences. From this step on, transmitter and receiver are assumed perfectly aligned (no channel distortions).

The third and last block deals with static polarization demultiplexing (*Demultiplexing*). This stage comprises Stokes-to-intensity transformation and *demapping matrix* application. Because both mentioned transformation matrices are known a priori, no real-time inversion is involved. The two aforementioned processes can be done separately, or they can be collapsed into a single pre-defined and static matrix multiplication. In both cases, the four SOPs are decoupled and the estimated transmitted intensity waveforms are retrieved. The inputs are the Stokes parameters at the output of the channel compensation step (*Channel distortion compensation*) irrespective of the approach:

1) *Two steps:* First, the input Stokes parameters are transformed into intensities through Eqs. (5). After that, the *demapping matrix* ($\mathbf{H}_{\mathbf{sys}}^{-\mathbf{1}}$ for $\mathbf{H}_{\mathbf{dist}} = I_2$) is applied.

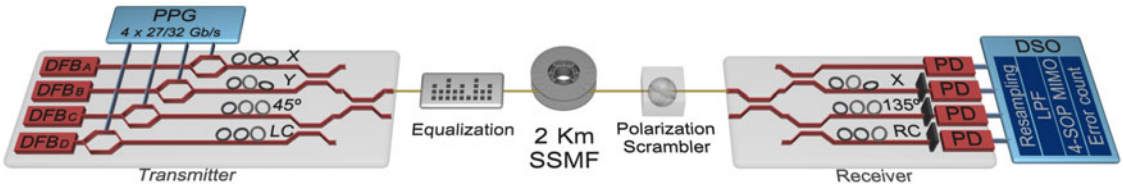

Fig. 3. Schematic of the experimental setup for 4-SOP 107 and 128 Gb/s transmission over 2-km SSMF. PPG: pulse pattern generator; DFB: distributed feedback laser; PD: photodiode; DSO: digital storage oscilloscope.

2) *One step:* The matrix 4 is converted to Stokes parameters, and its inverse is directly applied on the input Stokes parameters without intermediate, and exp conversion to intensity waveforms through Eqs. (5). For the particular transmitted SOP configuration shown in (4), the one demultiplexing matrix is given by:

$$\mathbf{M_{demux}} = \begin{pmatrix} 0.5 & 0.5 & -0.5 & -0.5 \\ 0 & 0 & 1 & 0 \\ 0.5 & -0.5 & -0.5 & -0.5 \\ 0 & 0 & 0 & 1 \end{pmatrix}. \quad (9)$$

The chain is ended with a single-threshold slicer and error counting (*Demodulation*) before forward error correction (FEC).

Note that other features/technologies can be added on top (e.g., nonlinear equalization for quadratic noise compensation or support for higher-order modulation formats) or in place (e.g., multi-dimensional clustering algorithms for joint Stokes vectors tracking) of the presented stages. However, the proof-of-concept experimental demonstration was realized with the strictly necessary modules for the sake of simplicity and worst-(non-optimum-)case evaluation.

III. Experimental Demonstration

The proposed 4-SOP IM/DD transmission subsystem was validated for two different baudrate configurations (4×27 GBd and 34×2 GBd for a net throughput of 100 and 120 Gb/s, respectively). Its performance is evaluated over 2-km SSMF in terms of bit-error rate (BER). Additionally, the stability of the SOP tracking algorithm is evaluated under stringent polarization change conditions [23]. This section contains the description of the experimental setup and the discussion on the collected results.

A. Testbed

Fig. 3 shows the schematic of the experimental setup. At the transmitter side, four distributed feedback lasers ($\mathrm{DFB_{A-D}}$) with 193.2–5 THz center frequencies are used as light sources. Frequency spacing is used to ensure incoherent power addition after their beating in the receiver's photodiodes.[4] The outputs of the DFBs are externally modulated with four integrated Mach–Zehnder modulators (MZM) with ∼30-GHz analog bandwidth. Note that the system exclusively requires intensity modulation, opening for the use of other external-modulation devices or direct-modulation techniques. The MZMs are electrically driven by two pulse pattern generator (PPG) modules, delivering a total of four independent 27 GBd (107 Gb/s; gross bitrate) or 32 GBd (128 Gb/s; gross bitrate) non-return-to-zero data streams with 3 *V*pp. Pseudorandom binary sequences of length $2^{15}-1$ are used, and fine symbol synchronization is attained with electrical delay lines. No DSP is employed at the transmitter. Finally, each of the modulated optical outputs from the MZMs is aligned to the chosen SOPs (*X*, *Y*, 45 and LC) with polarization controllers (PCs) and combined by means of standard 4×1 optical couplers.

The output from the transmitter is passed through a power equalization stage before fiber transmission. This stage comprises an erbium-doped fiber amplifier operated in saturation regime (∼5 dB noise figure) plus a variable optical attenuator. This structure allows for compensation of the disparate MZMs insertion losses in our transmitter, in no case providing input-output optical gain. After equalization, the signal is launched into 2-km SSMF for transmission. A polarization scrambler is installed at the end of the link for evaluating the performance of the polarization tracking algorithm.

At the receiver side, the signal is detected with a *Stokes analyzer* with ∼30 GHz analog bandwidth. The top branch (see Fig. 3) measures the instantaneous total power (*S0*), the other three include PCs and polarizers for realizing polarization filtering as described in Section II-D. After opto-electrical conversion in the photodiodes, the electrical signal is digitized by an 80-GS/s 25-GHz 3-dB BW real-time sampling scope (DSO) for later offline processing. The DSP at the receiver consists of the following modules: general front-end correction, Stokes-based compensation of the channel-induced polarization distortions plus demultiplexing, and error counting (see Section II-E for detailed explanation).

B. Results

Fig. 4(a) shows the BER performance of the system versus input power into the receiver for perfect polarization rotation compensation. Measured curves for both back-to-back (B2B) and transmission after 2-km SSMF are presented for the two cases of study, i.e., gross bitrates of 108 and 128

[4]For a given bandwidth per transmitted carrier, the laser frequency spacing will determine the degree of interference (after photodetection) from the higher-frequency beatings to the baseband components of interest. Insufficient separation will cause the higher-frequency beatings to fall within the photodiodes' analogue bandwidth and even partially overlap the baseband signal, with the resulting undesired distortion.Interference between non-orthogonal Jones vectors occurs when the lasers' frequency spacing ranges from dc to twice the analogue bandwidth of the photodiode. In non-severe cases, digital filtering (see Section II-E) can minimize the impact of the distortion. Severe cases may prevent correct signal demodulation, hence requiring the redesign of the frequency grid as first approach.

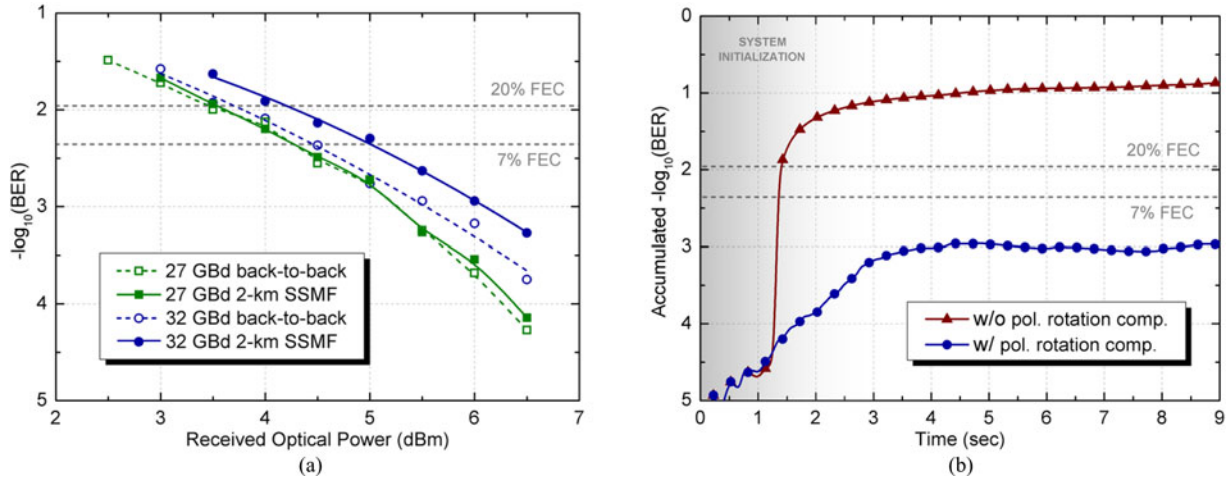

Fig. 4. (a) BER (∼2.9 million bits per point) versus received optical power for B2B and transmission configurations. (b) Accumulated BER versus time for 4-SOP 32 GBd transmission w/ and w/o pol rot. compensation algorithm.

Gb/s. Hard-decision 7% and 20% overhead FEC thresholds (4.4×10^{-3} and 1.1×10^{-2}, respectively) are depicted as reference.

Below-FEC transmission is attained for both 27 and 32 GBd irrespective of the overhead and the reach (B2B or transmission). For 27 GBd, the B2B receiver sensitivity at 100 Gb/s net bitrate (7% FEC) is ∼4.4 dBm, with no significant signal degradation or transmission penalty. The 32 GBd B2B case exhibits very similar performance to 27 GBd at the received power levels of interest (up to ∼5 dBm; right below-FEC region), with a minimum power sensitivity for 100 Gb/s net bitrate (20% FEC) of ∼3.7 dBm. Nevertheless, the transmission penalty after 2-km SSMF approaches ∼0.5 dB, thereby increasing the pre-FEC power sensitivity to a range comparable to that of 27 GBd 7% FEC. The observed similarity in the power budget margin could be argued to favor 4-SOPx27G over 4-SOPx32G in IM/DD scenarios targeting 100 Gb/s. This statement is based on the presumably lower latency and complexity of the 7% FEC, and the more relaxed constraints concerning the end-to-end bandwidth availability.

The experimental assessment of the Stokes-based polarization tracking algorithm is done with the help of an inline polarization scrambler. The fastest rotation rate the scrambler can achieve is on the order of radians per second, which is much slower than what can be detected within our DSOs maximum observation window. This means that, even using the maximum-available storage memory, one single frame could not capture fast enough transitions to evaluate the software in realistic polarization-change conditions. Therefore, short traces are periodically stored, where the period time determines the equivalent polarization rotation speed observed by the system (for fixed scrambler settings). After calculating the rotation matrix based on one set of frames, it remains constant during the mentioned storage period. This pseudo-continuous (fast periodic) routing, allows scrambler-independent software testing for flexible rotation speeds. Particularly in our experimental characterization, a total of 120 frames of 16 000 bits each were processed every 75 ms (9 s), resulting in an equivalent angular speed in the order of Mrad/s. The maximum *SOP tracking* convergence depth was set to 2000 samples.

Fig. 4(b) illustrates the accumulated BER over time for the 4-SOPx32GBd configuration at 25.5 dB SNR per symbol, subjected to the aforementioned microsecond-timescale polarization rotations. This particular case is deemed representative of worst/poor-case system performance. The results show stable $\sim 10^{-3}$ BER after system initialization, which is achieved by forcing perfect transmitter-receiver alignment during the first frames. The curves obtained with and without the polarization tracking algorithm clearly show: (i) the need for rotation compensation to accomplish correct signal recovery and (ii) the successful and stable below-FEC performance achieved with the proposed algorithm under conditions far more demanding than can be expected in 2-km SSMF transmission links [23].

IV. Conclusion

We have presented the first experimental demonstration of an IM/DD optical subsystem that simultaneously uses four distinct SOP for transmitting four independent data streams. This demonstration goes beyond both the traditional approach to polarization multiplexing (*X* and *Y*) and the common belief that the potential number of simultaneous polarizations in such a link is three at most. Our approach has the potential to be used alongside or in place of existing technologies (e.g., WDM or advanced modulation formats) for simplification of the receiver structure or per-channel capacity increase. The DSP at the receiver operates on the Stokes space to account for general polarization states, their rotation during transmission, and proper demultiplexing upon reception. In fact, operating in Stokes space is what allows tracking and compensation of polarization rotation without requiring any phase information with low computational load, which enables application in real scenarios. The system is validated for two different baudrate configurations, i.e. 4 × 27 GBd (108 Gb/s) and 4 × 32 GBd (128 Gb/s). Transmission below FEC limit is shown for both cases over 2-km SSMF at a center wavelength of 1550 nm.

APPENDIX
4-SOP DSP SCHEMA

1) Signal conditioning
   - Resampling.
   - Matched/low-pass filtering.
2) Front-end correction
   - Time skew.
   - Photodiodes' (PD) responsivity normalization.
   - Direct current (DC) offset.
3) Stokes space processing
   - Intensity vectors to Stokes parameters conversion (see Eqs. (5)).
   - Timing recovery and decimation from Stokes parameters.
   - Polarization tracking.
     i Zero-power discriminator: find and demodulate/store trivial zero-power cases.
     ii Normalize Stokes parameters by *S0*.
     iii Initialize the channel's Mueller matrix if needed. *START LOOP*
     iv Estimate/update decision thresholds on the normalized Stokes parameters (see Fig. 2).
     v Evaluate one normalized Stokes parameter.
     - $\sim \pm 1$. Calculate the sign-dependent error signal and update the values (S_{ij}) of the channel's Mueller matrix ($\mathbf{M_{dist}}$) (see [17] for the mathematical formulation of the error signal and the update rule). *START LOOP.*
     - ~ 0. Restart the evaluation step for the next normalized Stokes parameter.

     END LOOP (iterate until convergence)
   - Channel distortion compensation
     i) Transpose the estimated channel matrix ($\mathbf{M_{dist}^{-1}} = \mathbf{M_{dist}^{T}}$) and apply it to the received Stokes parameters to compensate for the channel distortions.
4) Demultiplexing (either *two-step* or *one-step* approach. See Section II-E *Demultiplexing*).
5) Demodulation.

ACKNOWLEDGMENT

The authors would like to thank A. Tatarczak, S. Saldaña, and R. Borkowski for the technical support and helpful comments.

REFERENCES

[1] J. Estarán, M. A. Usuga, E. Porto da Silva, M. Piels, M. Iglesias Olmedo, and I. Tafur Monroy, "Quad-polarization transmission for high-capacity IM/DD links," presented at the European Conf. Optical Communication, Cannes, France, 2014, p. PDP.4.3.

[2] A. D. Kersey, M. J. Marrone, and A. Dandridge, "Polarization diversity detection for fiber interferometers using active feedback control of output polarization-mode selection," *Opt. Lett.*, vol. 15, no. 22, pp. 1315–1317, Nov. 1990.

[3] Y. Han and G. Li, "Coherent optical communication using polarization multiple-input-multiple-output," *Opt. Exp.*, vol. 13, no. 19, pp. 7527–7534, 2005.

[4] C. Herard and A. Lacourt, "Three channel multiplexing using polarization of light," *Opt. Commun.*, vol. 60, nos. 1/2, pp. 27–31, Oct. 1986.

[5] R. Rodes, M. Mueller, B. Li, J. Estarán, J. Jensen, T. Gruendl, M. Ortsiefer, C. Neumeyr, J. Rosskopf, K. Larsen, M. Amann, and I. Monroy, "High-speed 1550 nm vcsel data transmission link employing 25 GBd 4-PAM modulation and hard decision forward error correction," *J. Lightw. Technol.*, vol. 31, no. 4, pp. 689–695, Feb. 2013.

[6] J. Lee, N. Kaneda, T. Pfau, A. Konczykowska, F. Jorge, J.-Y. Dupuy, and Y.-K. Chen, "Serial 103.125-gb/s transmission over 1 km SSMF for low-cost, short-reach optical interconnects," presented at the Optical Fiber Communication Conf., San Francisco, CA, USA, Mar. 2014.

[7] T. Tanaka, M. Nishihara, T. Takahara, W. Yan, L. Li, Z. Tao, M. Matsuda, K. Takabayashi, and J. Rasmussen, "Experimental demonstration of 448-Gbps+ DMT transmission over 30-km SMF," presented at the Optical Fiber Communication Conf., 2014, p. M2I.5.

[8] W. Yan, T. Tanaka, B. Liu, M. Nishihara, L. Li, T. Takahara, Z. Tao, J. Rasmussen, and T. Drenski, "100 gb/s optical IM-DD transmission with 10G-class devices enabled by 65 gsamples/s CMOS DAC core," presented at the Optical Fiber Communication Conf., Anaheim, CA, USA, Mar. 2013.

[9] X. Xiao, F. Li, J. Yu, Y. Xia, and Y. Chen, "Real-time demonstration of 100 gbps class dual-carrier DDO-16QAM-DMT transmission with directly modulated laser," presented at the Optical Fiber Communication Conf., San Francisco, CA, USA, Mar. 2014.

[10] M. I. Olmedo, T. Zuo, J. B. Jensen, Q. Zhong, X. Xu, S. Popov, and I. T. Monroy, "Multiband carrierless amplitude phase modulation for high capacity optical data links," *J. Lightw. Technol.*, vol. 32, no. 4, pp. 798–804, Feb. 2014.

[11] J. D. Ingham, R. V. Penty, I. White, and D. G. Cunningham, "100 Gb/s PAM4-CAP2 real-time modulation of a single optical source for next-generation datacommunication links," presented at the Optical Fiber Communication Conf., San Francisco, CA, USA, 2014, vol. 1, p. W1F.1.

[12] A. Al Amin, H. Takahashi, I. Morita, and H. Tanaka, "100-Gb/s direct-detection OFDM transmission on independent polarization tributaries," *IEEE Photon. Technol. Lett.*, vol. 22, no. 7, pp. 468–470, Apr. 2010.

[13] D. Qian, N. Cvijetic, J. Hu, and T. Wang, "108 Gb/s OFDMA-PON with polarization multiplexing and direct detection," *J. Lightw. Technol.*, vol. 28, no. 4, pp. 484–493, Feb. 2010.

[14] C. Li, H. Li, Q. Yang, M. Luo, X. Zhang, R. Hu, Z. Li, W. Li, and S. Yu, "Single photodiode direct detection system of 100-Gb/s OFDM/OQAM-64QAM over 80-km SSMF within a 50-GHz optical grid," *Opt. Exp.*, vol. 22, no. 19, pp. 22 490–22 497, Sep. 2014.

[15] M. Nazarathy, and A. Agmon, "Doubling direct-detection data rate by polarization multiplexing of 16-QAM without active polarization control." *Opt. Exp.*, vol. 21, no. 26, pp. 31 998–32 012, Dec. 2013.

[16] D. Che, A. Li, X. Chen, Q. Hu, Y. Wang, and W. Shieh, "160-Gb/s stokes vector direct detection for short reach optical communication," presented at the Optical Fiber Communication Conf., 2014, p. Th5C.7.

[17] K. Kikuchi, "Electronic polarization-division demultiplexing based on digital signal processing in intensity-modulation direct-detection optical communication systems." *Opt. Exp.*, vol. 22, no. 2, pp. 1971–1980, Jan. 2014.

[18] K. Kikuchi and S. Kawakami, "16-ary stokes-vector modulation enabling DSP-based direct detection at 100 Gbit/s," presented at the Optical Fiber Communication Conf., San Francisco, CA, USA, 2014, p. Th3K.6.

[19] K. Kikuchi and S. Kawakami, "Multi-level signaling in the stokes space and its application to large-capacity optical communications." *Opt. Exp.*, vol. 22, no. 7, pp. 7374–7387, Apr. 2014.

[20] M. Chagnon, M. Poulin, S. Lessard, and D. V. Plant, "1 λ 224 Gb/s 10 km transmission of polarization division multiplexed PAM-4 signals using 1.3 μm SiP intensity modulator and a direct-detection MIMO-based receiver," presented at the European Conf. Optical Commun., 2014, p. PDP.4.4.

[21] C. Brosseau, *Fundamentals of Polarized Light: A Statistical Optics Approach*. New York, NY, USA: Wiley, 1998.

[22] C. Herard and A. Lacourt, "New multiplexing technique using polarization of light." *Appl. Opt.*, vol. 30, no. 2, pp. 222–231, Jan. 1991.

[23] P. Krummirich and K. Kotten, "Extremely fast (microsecond timescale) polarization changes in high speed long haul WDM transmission systems," presented at the Optical Fiber Communication Conf., Los Angeles, CA, USA, 2004.

[24] B. Szafraniec, B. Nebendahl, and T. Marshall, "Polarization demultiplexing in stokes space." *Opt. Exp.*, vol. 18, no. 17, pp. 17 928–17 939, Aug. 2010.

[25] H. Meyr, M. Moeneclaey, and S. Fechtel, *Digital Communication Receivers: Synchronization, Channel Estimation, and Signal Processing*. New York, NY, USA: Wiley, 1997.

Authors' biographies not included at authors request due to space constraints.